ACS APPLIED MATERIALS & INTERFACES

Research Article

www.acsami.org

"Insensitive" to Touch: Fabric-Supported Lubricant-Swollen Polymeric Films for Omniphobic Personal Protective Gear

Viraj G. Damle,[†] Abhishiktha Tummala,[†,⊥] Sriram Chandrashekar,[†,⊥] Cassidee Kido,[†,⊥] Ajay Roopesh,[†] Xiaoda Sun,[†] Kyle Doudrick,[‡] Jeff Chinn,[§] James R. Lee,[∥] Timothy P. Burgin,[∥] and Konrad Rykaczewski*[,†]

[†]School for Engineering of Matter, Transport and Energy, Arizona State University, Tempe, Arizona 85287, United States

[‡]Department of Civil and Environmental Engineering and Earth Sciences, University of Notre Dame, Notre Dame, Indiana 46556, United States

[§]Integrated Surface Technologies, Inc., Menlo Park, California 94025, United States

[∥]Naval Surface Warfare Center Dahlgren Division, Dahlgren, Virginia 22448, United States

Supporting Information

ABSTRACT: The use of personal protective gear made from omniphobic materials that easily shed drops of all sizes could provide enhanced protection from direct exposure to most liquid-phase biological and chemical hazards and facilitate the postexposure decontamination of the gear. In recent literature, lubricated nanostructured fabrics are seen as attractive candidates for personal protective gear due to their omniphobic and self-healing characteristics. However, the ability of these lubricated fabrics to shed low surface tension liquids after physical contact with other objects in the surrounding, which is critical in demanding healthcare and military field operations, has not been investigated. In this work, we investigate the depletion of oil from lubricated fabrics in contact with highly absorbing porous media and the resulting changes in the wetting characteristics of the fabrics by representative low and high surface tension liquids. In particular, we quantify the loss of the lubricant and the dynamic contact angles of water and ethanol on lubricated fabrics upon repeated pressurized contact with highly absorbent cellulose-fiber wipes at different time intervals. We demonstrate that, in contrast to hydrophobic nanoparticle coated microfibers, fabrics encapsulated within a polymer that swells with the lubricant retain the majority of the oil and are capable of repelling high as well as low surface tension liquids even upon multiple contacts with the highly absorbing wipes. The fabric supported lubricant-swollen polymeric films introduced here, therefore, could provide durable and easy to decontaminate protection against hazardous biological and chemical liquids.

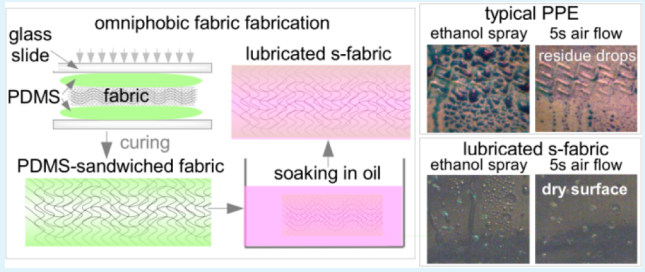

KEYWORDS: *superhydrophobic/philic surfaces, lubricated omniphobic surfaces, functional coatings, hybrid personal protective gear*

1. INTRODUCTION

Personal protective gear used in healthcare and military applications is intended to separate a person from hazardous fluids in the surrounding because their penetration into the suit could have dire consequences. For example, human contact with even a small volume of liquid contaminated with biological threats such as the Ebola virus or chemical weapon agents (CWAs) such as Sarin can be deadly.[1,2] Both of these liquids pose a threat not only as macroscale drops but also as aerosols with microscale droplets.[1,2] In addition, Sarin and other types of CWAs are low surface tension organic liquids with a low vapor pressure (i.e., they can wet the majority of common materials and do not evaporate readily, so they are likely to remain in the liquid phase).[1] As a result, by staying on surfaces, CWA microdroplets can readily be absorbed into different types of materials. Consequently, slow off-gassing of these dangerous chemicals from contaminated gear away from the direct exposure zone also poses a major health threat.[3,4] Thus, the use of personal protective gear made from omniphobic materials that easily shed droplets of all sizes could provide enhanced protection from most hazardous liquids within a direct exposure zone, as well as facilitate postexposure decontamination of the gear.

Since microporous polytetrafluoroethylene (PTFE) fibers were introduced in the early 1970s,[5] most of the modern liquid repelling fabrics have been made of low surface energy materials with nano- and microscale morphology.[6−14] The resulting materials can have superhydrophobic properties manifested through sessile water drops with a static contact angle greater than 150° and contact angle hysteresis (CAH) below 10° (CAH is the difference between the contact angle the liquid makes while advancing and receding from the surface).[15,16] The

Received: December 3, 2014
Accepted: January 29, 2015
Published: January 29, 2015

DOI: 10.1021/am5085226
ACS Appl. Mater. Interfaces 2015, 7, 4224−4232

low adhesion of water drops residing on top of these materials stems from a composite liquid−fabric interface that includes air cavities (i.e., the nonwetting Cassie−Baxter state).[17] A combination of low surface energy fibers with re-entrant geometry can also be used to make oleophobic[18−21] and even omniphobic[22−25] fabrics that repel liquids with surface tension down to ∼25 and ∼15 mN/m, respectively. However, textured superhydrophobic surfaces are easily wetted by low surface tension liquids, while omniphobic surfaces with re-entrant texture can be flooded during condensation.[26] Furthermore, the latter surfaces have been demonstrated to shed macroscale drops of low surface tension liquid but might be penetrated by a mist and/or spray with microscale droplets whose sizes are comparable to that of the texture.

Lubricated textured materials, on the other hand, can overcome some of the challenges posed by textured omniphobic materials by replacing the air trapped within cavities of the surface roughness with a low surface energy lubricant. This oil impregnated into the fabric must be immiscible and must not react with any of the liquids that the material is supposed to repel.[27,28] Lubricated materials, in general, have been reported to possess self-cleaning, self-healing, and omniphobic properties[27−30] and have been proposed for numerous applications, including condensation rate enhancement,[26,31−34] frost prevention,[35−37] ice,[35,38,39] bacteria,[40,41] and salt scale[42] accumulation, as well as reduction of drag and drop adhesion[43−47] and most recently manipulation of individual[48] and composites drops.[49,50] Shillingford et al.[51] recently extended the concept of lubricated surfaces to lubricated fabrics. Specifically, they demonstrated that omniphobic fabrics can also be achieved by impregnating a lubricant into microfibers coated with hydrophobic nanoparticles.

Durability is a key issue for fabrics since their expected use involves constant mechanical perturbation of the material. To simulate fabric wear expected in typical applications, Shillingford et al.[51] performed two types of durability tests. In the first set of experiments, the authors observed how rubbing nonlubricated nanoparticle coated fabrics with a wipe affects the ability of the material to repel water. They found that the rubbing action induced some damage to the nanoparticle coating but did not affect the hydrophobic characteristics of the fabrics. In the second set of experiments, Shillingford et al.[51] evaluated how water drop sliding angle is affected by repeated twisting of lubricated nanoparticle coated fabrics. In a majority of the cases, twisting induced damage to the nanoparticle coating and increased the water sliding angle. However, the ability of the lubricated fabrics to shed low surface tension liquids (i.e., remain omniphobic) during a typical application has not been tested. In addition to failure due to physical damage to the fibers' coating, omniphobic characteristics of lubricated materials can also be compromised by oil depletion. For example, the anti-icing performance of the lubricated nanotextured surfaces was found to degrade during frosting−defrosting cycles due to the rapid draining of the lubricant into a growing network of nanoicicles.[36] This observation raises a key question about performance of lubricated fabrics: *Can the lubricant be wicked away from the fabric when brought into contact with other materials (e.g., a second fabric, a wall, a chair, or in the case of military operations, sand)? If so, what is the impact of lubricant depletion on the fabric's liquid-repelling characteristics*?

In this work, we investigate the depletion of lubricant from impregnated fabrics in contact with highly absorbing porous media and the resulting changes in the wetting characteristics of the fabrics by representative low and high surface tension liquids. In particular, we quantify the loss of the lubricant and the dynamic contact angles of water and ethanol on lubricated fabrics upon repeated pressurized contact with highly absorbent cellulose-fiber wipes at different time intervals. We demonstrate that, in contrast to hydrophobic nanoparticle coated microfibers, fabrics encapsulated within a polymer that swells with the lubricant retain the majority of their oil and have the ability to easily shed water and ethanol, even after having multiple contacts with the high absorbing wipes.

2. EXPERIMENTAL SECTION

2.1. Specimen Fabrication. "Home décor" 100% cotton and "Black Silk Essence" 100% polyester (PET) obtained from the Jo-Ann Fabrics store in Tempe, AZ, were used for the experiments in this study (see Figure 1A,B). The fabrics were cut into 2.5 cm by 2.5 cm square pieces and washed thoroughly using water and ethanol. Subsequently, the fabrics were dried for 30 min using compressed air flow and heated at 90 °C. To produce six fabric architectures, the 100% cotton and 100% PET were modified in three different routes. Specifically, these base fabrics were either conformally coated with hydrophobic alumina nanoparticles (referred to as NP-cotton and NP-PET samples), vacuum infused with polydimethylsiloxane (PDMS) (i-cotton and i-PET), or sandwiched in-between PDMS with nearly flat exterior surfaces (s-cotton and s-PET). To produce a solid polymeric coating, the fabrics treated with a mixture of uncrosslinked PDMS and a cross linking agent were thermally cured. After fabrication, all samples were lubricated by soaking in silicone oil (see Section 2.2 below for details). We note that control experiments were also conducted on bare fabrics and fabrics coated with both nanoparticles and solid PDMS. The latter sample was fabricated by encapsulating fabrics already coated with nanoparticles into a solid PDMS matrix (see details of the individual fabrication processes below). Both water and ethanol wicked into the base fabrics even after they were soaked in silicone oil. In turn, the presence of nanoparticle coating under the PDMS coating did not have any noticeable effects on oil absorption and retention as well as wetting properties of the composite material. Consequently, bare fabrics and double coated fabrics were not studied further (see the Supporting Information for further details).

For PDMS treatment of the fabric, we used Sylgard 184 (Dow Corning). The PDMS elastomer base and curing agent were mixed in a ratio of 10:1 (by mass). Mixing of the two components was followed by vacuum degassing for about 15 min to remove air bubbles. To vacuum infuse the fabrics with PDMS, about 0.5 g of the degassed PDMS mixture was applied on the top surface of the fabrics placed in a filtration funnel (FT-0010-034, CTechGlass) that was connected to a vacuum pump (Edwards RV5). Vacuum infusion was continued until the PDMS mixture was not visible on the fabric's surface. The final fabrication step for the i-cotton and i-PET samples was thermal curing on a hot plate preheated to 90 °C for 90 min. To fabricate the sandwiched specimen (s-cotton and s-PET), about 2 g of the PDMS mixture was spread onto two flat precleaned glass slides. A piece of the fabric was put on top of the bottom glass slide−PDMS mixture stack and subsequently covered with the other PDMS mixture−glass slide stack. A 10 g weight was used to lightly press the elastomer mixture into the fabric. The entire assembly was then moved to the hot plate for 90 min of thermal curing at 90 °C. After this process, the fabric sandwiched or "encapsulated" in the cured PDMS polymer was removed from in-between the slides. To fabricate the PDMS slabs with thickness comparable to that of cotton and polyester (500 and 100 μm), about 1 g of the PDMS mixture was applied to the center of a glass slide. Two pieces of the same fabrics were placed on either side of the PDMS mixture to set the appropriate height for the slab. Next, a second glass slide was gently placed on top of the PDMS and the fabrics. The thin PDMS slides were thermally cured and cut with scissors to a size of 2.5 cm by 2.5 cm. To fabricate the 2 mm thick PDMS slab, a 3D printed ABS rectangular base dish was filled with the

DOI: 10.1021/am5085226
ACS Appl. Mater. Interfaces 2015, 7, 4224−4232

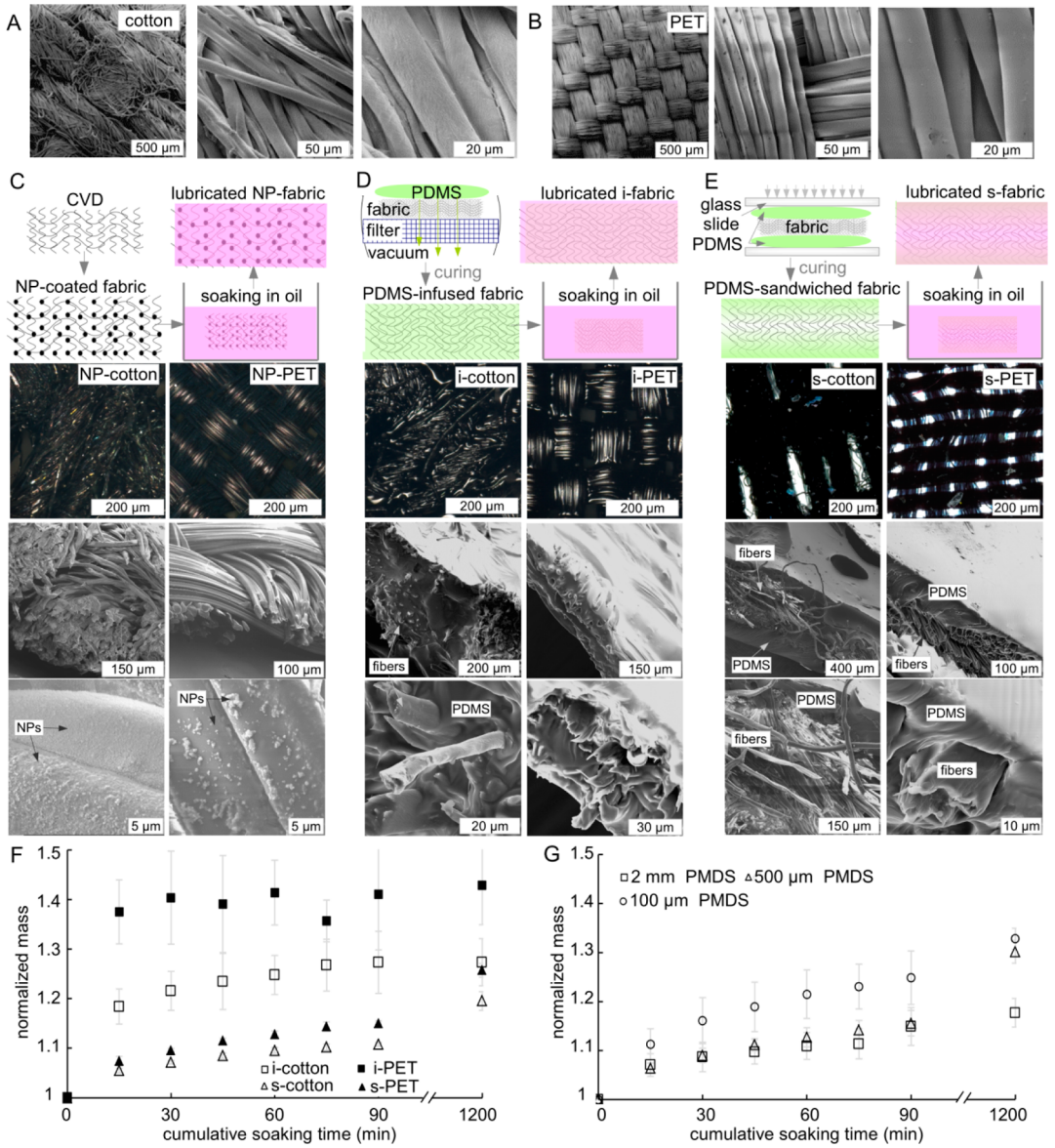

Figure 1. Optical and SEM images of densely woven (A) cotton and (B) polyester (PET) fabrics prior to modification, (C–E) fabrication process schematics of top-down postfabrication optical images and cross-sectional postfabrication SEM images of cotton and PET (C) nanoparticle coated (NP-) fabrics, (D) vacuum PDMS infused (i-) fabrics, and (E) PDMS sandwiched (s-) fabrics (i.e., fabrics supported PDMS slabs); images show samples prior to soaking with silicone oil; (F–G) measured silicone oil absorption quantified in terms of normalized soaked mass ($\bar{m}_s$)for the (F) fabrics and (G) flat PDMS slabs with thickness comparable to the fabrics.

PDMS mixture, which was subsequently thermally cured. Images in Figures 1 and S1, Supporting Information, show the morphologies of the i-cotton, i-PET, s-cotton, and s-PET samples prior to soaking in oil.

In order to fabricate the nanoparticle coated fabrics (NP-cotton and NP-PET), the prewashed and dried fabrics were conformally coated by alumina nanoparticles encapsulated in a silica matrix using RPX-540 manufactured by Integrated Surface Technologies, Inc. Specifically, the fabrics were conformally coated by nanoparticles synthesized in the vapor phase reaction of trimethylaluminum and water. The precipitated nanoparticles were encapsulated in a thin silicon oxide matrix via atomic layer deposition. Subsequently, the surfaces were modified with a vapor phase deposition of tridecafluoro-1,1,2,2-tetrahydrooctyltrichlorosilane. Silicon wafers modified using this coating have a water contact angle of 111° ± 4°.[52]

2.2. Measurement of Oil Absorption during Soaking. The specimens were soaked in 10 mL of 100 cSt silicone oil at 15 min intervals. Between each soaking interval, the samples were removed from the oil and hanged vertically in air for 5 min to remove excess oil from the surface. The PDMS samples were also put in between two absorbing cellulose fiber wipes (Kimwipes from Kimberly Clark) with areas identical to that of the fabrics and then pressed gently with a 10 g weight for 10 s. After this procedure, the samples were weighed using the electronic weight scale (FA2004 with 0.0001 g resolution). This procedure was repeated 6 times (2 h experimental duration and 1.5 h cumulative soaking time). In addition, samples were allowed to soak in oil for 20 h to see how much more oil they absorbed when compared to the 1.5 h soaking time. Each oil absorption measurement was repeated six times, with a new specimen for each trial. We reported average values with uncertainty calculated using the two-tailed T-student's distribution, with a 95% confidence interval.

2.3. Measurement of Oil Depletion during Contact with Absorbing Media. The specimens were soaked in 10 mL of 100 cSt silicone oil for 2 h to saturate the samples with oil. Excess oil was then removed from the fabric surface using the same procedure as described in Section 2.2. The contact experiments were conducted on the saturated specimen by placing the samples between two absorbing

DOI: 10.1021/am5085226
ACS Appl. Mater. Interfaces 2015, 7, 4224–4232

wipes and then pressing on them using a 200 g weight at preset time intervals of 30 or 60 s. After each time interval, used wipes were replaced with new ones and the same specimen was again pressed against the wipes for the same time interval. This procedure was repeated 2 and 4 times or 5 and 10 times for preset times of 30 and 60 s, respectively.

2.4. Contact Angle Measurement. A home-built goniometer, composed of a stage 3D printed using Makerbot Replicator 2x, a CCD camera (Imaging Source DFK23U618) with high magnification lens (Navitar 6232A), a syringe pump (New Era Pump System NE-1000), and a light source (Dolan-Jenner MH-100), was used to measure the static and dynamic contact angles of water and ethanol on all the specimens. The liquid was gradually dispensed and retracted using a syringe pump. The specimen was kept on the stage and illuminated via the diffused light source. Images captured during the experiment were stored and analyzed using ImageJ software.[53] Specifically, separate images were chosen to calculate six advancing (θ_{a1}, θ_{a2}, ..., θ_{a6}) and six receding (θ_{r1}, θ_{r2}, ..., θ_{r6}) contact angles. Average advancing and receding contact angle, θ_a and θ_r, respectively, were calculated using these values. The uncertainty values in θ_a (σ_{θ_a}) and θ_r (σ_{θ_r}) were calculated considering a two-tailed T-student's distribution with 90% confidence interval. Average contact angle hysteresis was later computed as CAH = $\theta_a - \theta_r$ with $\sigma_{CAH} = ((\sigma_{\theta_a})^2 + (\sigma_{\theta_r})^2)^{1/2}$. The measured static and dynamic contact angles are presented in Table S1 and Figure S2, respectively, in the Supporting Information. For the wipe contact experiments, the contact angle measurements were performed within ~30 min from the time that the wipes were removed. To ensure that the dynamics of oil diffusion to the surface did not affect the observed CAH, we measured the CAH of water on s-cotton samples right after, 5, 10, and 30 min after 5 sequential 1 min contact experiments (our "initial" data point is offset by ~1 to 3 min from the time that the wipes were removed). The water CAH values for "0", 5, 10, and 30 min points were 16° ± 4°, 18° ± 4°, 19° ± 4°, and 17° ± 3°, respectively. Thus, relubrication of the PDMS surface after pressing with a wipe likely occurs faster than ~1 min and should not impact our CAH measurements.

2.5. Ethanol Spraying and Air-Blowing Experiments. In order to conduct the ethanol spray experiments, 5 cm by 5 cm square pieces of s-cotton and NP-cotton were fabricated using the procedures described in Section 2.1. A 5 cm by 5 cm square piece of a thick nitrile rubber acid-protection glove (Mcmaster-Carr) was used as a reference sample. Slightly smaller square pieces of cellulose wipes were placed behind the specimen before the stack was fixed to a vertical surface using an electrical insulation tape. Control experiments were conducted to ensure that the cellulose wipes were not directly exposed to the ethanol spray and were not stained by ethanol wicking in from the edges of the samples. Ethanol was dyed blue using methylene blue (Sigma-Aldrich) and sprayed continuously onto the specimen as a fine mist for 5 s and from a distance of about 30 cm using a Light Duty Hand Pump Sprayer with 1.4 L capacity (McMaster-Carr). Later, ethanol was removed from the specimen by blowing compressed air over the specimen for 5 to 10 s. After completing the experiment, excess ethanol was carefully wiped from the area surrounding the specimen. Subsequently, the samples were carefully removed to expose the wipes mounted behind them.

3. RESULTS AND DISCUSSION

We tested six fabric architectures consisting of densely woven 100% polyester (PET) or 100% cotton with ~10−15 μm diameter fibers modified using three different solid coatings prior to soaking in silicone oil. These two base fabrics were selected because Shillingford et al.[51] have shown that densely woven microfibers provide most robust omniphobic characteristics when coated by hydrophobic nanoparticles and soaked in a lubricant. The base cotton and PET fabrics had varying topology with the PET fibers closely aligned with the direction of the weave while the cotton fibers were more randomly dispersed (see Figure 1A,B). To provide an architecture similar to the nanoparticle coated fabrics described by Shillingford et al.,[51] the base fabrics were conformally coated via vapor-phase deposition of ceramic nanoparticles and thin locking matrix (see the fabrication schematic and images of NP-cotton and NP-PET samples in Figure 1C). This treatment was followed by vapor-phase hydrophobization of the entire sample.[52] Silicon and metal substrates modified using this procedure have been previously used as a robust base for stable lubricated materials for anti-icing[36] and condensation enhancement applications.[26]

As an alternative to the lubricated NP-coated fabrics, we modified the two base fabrics with a polymer that can readily absorb and swell with a variety of oils. Our hypothesis was that the use of such lubricant swollen polymer coating will decrease the oil release rate upon contact with other porous solids. Fabrics that retain more oil should have more robust omniphobic characteristics. We selected PDMS as the polymer coating because its swelling behavior is well-known to significantly slow down the release of a variety of oils.[41,54−61] The release dynamics of oils from oil-soaked PDMS paints have been investigated during biofouling experiments since the late 1970s.[41,54−61] In addition to slowing down release of the lubricant, the use of an elastic polymer instead of a nanoceramic should also reduce the potential for cracking in the fiber's coating reported by Shillingford et al.[51] From an application perspective, the use of fabric and polymer combination instead of just a free-standing polymer film is beneficial because the woven fibers provide a robust backbone to the otherwise relatively fragile and thin (~100 to ~500 μm) PDMS film. We combined PDMS and the fabrics along two routes. The first route produced a composite fabric with topography closely following that of the original fiber weave. We achieved this by forcing the PDMS mixture into the fabrics with vacuum infusion (see the fabrication schematic and images of the i-cotton and i-PET samples in Figure 1D). Conversely, the second fabrication route resulted in elastomer penetration primarily around the outer fibers and, with the exception of a few residual craters resulting from trapped air bubbles, a smooth exterior surface (see the fabrication schematic and images of the s-cotton and s-PET samples in Figure 1E). We fabricated this type of sample architecture by thermally curing fabrics sandwiched between two glass slides covered with the PDMS mixture. Since this PDMS modification essentially creates fabrics encapsulated in a PDMS film, we refer to them as fabric-supported PDMS films. In addition to the fabric containing samples, we also made pure PDMS slabs with flat exterior surfaces and thicknesses of 100 μm, 500 μm, and 2 mm. In all cases, the PDMS solution was cured for 1.5 h at 90 °C to create the solid PDMS matrix for subsequent oil impregnation.

In order to complete fabrication of the lubricated fabrics, all the specimens were soaked in a 100 cSt silicone oil bath. After soaking, the excess oil was removed by hanging the samples vertically for 5 min and gently pressing the surface of the samples against a cellulose fiber wipe for 10 s with a pressure of ~270 Pa (10 g mass over ~3.6 cm^2 area). We note that the latter step was not performed for the nanoparticle coated fabrics because we found that even this brief procedure could remove oil from within the fabric. For absorption measurements, the soaking procedure followed by weighting was repeated at 15 min soaking intervals for a cumulative total soaking time of 1.5 h for each sample. As a reference, the mass of the samples was also checked after a 20 h soaking period. The plots in Figure 1F,G show a normalized soaked sample

DOI: 10.1021/am5085226
ACS Appl. Mater. Interfaces 2015, 7, 4224−4232

mass ($\bar{m}_s$) that we defined as the soaked sample mass divided (m_s) by the dry sample mass (m_d) for different cumulative soaking times. The i-cotton and i-PET samples had significantly higher $\bar{m}_s$ than the s-cotton and s-PET samples as well as the plain PDMS slabs with comparable thickness to the fabrics. The i-cotton and i-PET samples also were saturated with the oil within the first 30 min of soaking, while the other samples showed another ∼0.05 to 0.1 increase in $\bar{m}_s$ after the extended 20 h soaking. However, since the rate of silicone oil absorption was about 10 times slower in the later soaking stages for the latter samples, we capped the soaking time at 1.5 to 2 h for all the subsequent experiments. The nanoparticle coated samples impregnated rapidly with the oil to reach a normalized soaked mass of 1.87 ± 0.03 and 1.81 ± 0.11 for the NP-cotton and NP-PET samples, respectively (soaking time did not affect the $\bar{m}_s$). All coated fabrics were hydrophobic prior to soaking in the lubricant. However, the nanoparticle-coated fabrics were penetrated by ethanol, while the surfaces of the fabrics modified with a solid PDMS matrix were partially to fully wetted by the ethanol. Lubrication rendered all the fabrics omniphobic with CAH less than about 5° for both of the liquids. The measured static and dynamic contact angles are presented in Table S1 and Figure S2, respectively, Supporting Information.

To estimate the fabrics' wetting characteristics upon contact with other objects, we placed the samples soaked in silicone oil between two cellulose fiber wipes (see schematic in Figure 2A and SEM images of the wipes in Figure 2B). We selected these highly absorbing wipes to provide a very conservative, "worst-case" scenario estimate of the lubricated fabric performance (could be representative of fabric on a chair). To simulate the typical force exerted by a person in contact with an object, we used a weight placed on the top cellulose fiber wipe to induce additional pressure on the sample. The average surface areas of human bodies are on the order of ∼1.5 to ∼2 m^2 for adult females and males, while the average corresponding weights are ∼60 and ∼70 kg, respectively.[62] Thus, persons resting completely flat on their backs would exert a pressure of ∼700 Pa. However, a person may also touch objects by partial contact, for example, during sitting or resting against a wall. To account for this possibility, we applied ∼8 times higher pressure of ∼5400 Pa by placing 0.2 kg over the ∼3.6 cm^2 surface area of the top cellulose wipe. As schematically illustrated in Figure 2A, we conducted the experiments by bringing the fabrics in contact with the wipes for intervals of 30 and 60 s with up to 10 contact instances. To avoid artifacts caused by saturated fibers, fresh wipes were used for each individual contact experiment. Prior to these experiments, we also tested whether or not this pressing procedure damaged the nanoparticle coating. The SEM images in Figure 2C show that, in contrast to twisting and rolling, pressing the NP-fabrics did not degrade the fiber nanoparticle coatings. The morphology of the solid PDMS-modified fabrics was not affected by pressing, bending, or twisting (see the Supporting Information for further details).

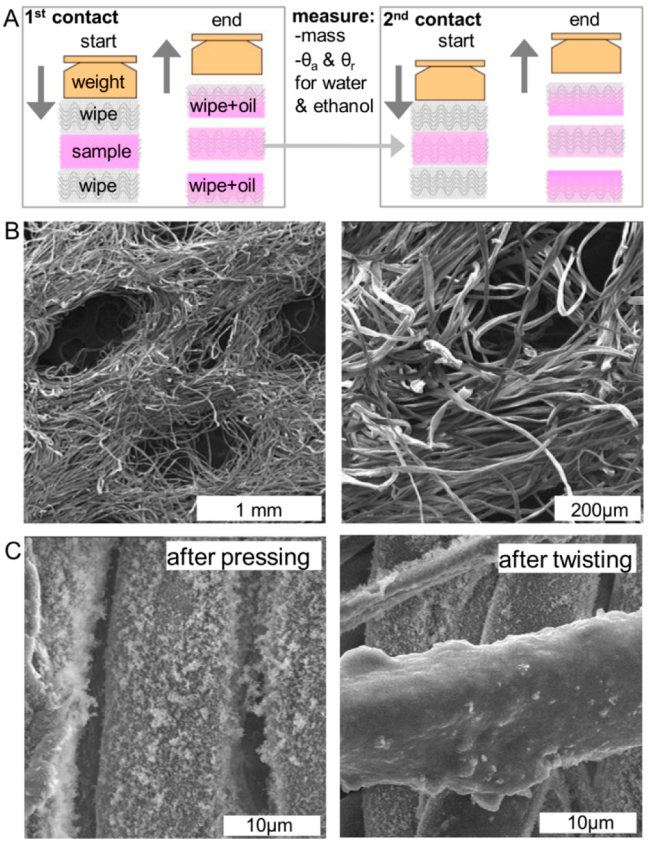

Figure 2. (A) Schematic of the multiple contact experiments with silicone oil and the absorbing cellulose wipes depicted in pink and gray, respectively, (B) SEM images of the cellulose wipes, and (C) SEM images of nanoparticle coated cotton fibers after pressing (no damage) and twisting (visible damage).

The plots in Figure 3A,B show lubricant loss induced by multiple contact experiments for lubricated fabrics and, as a reference, oil-soaked PDMS slabs. We quantified the results in terms of normalized sample mass after contact ($\bar{m}_c$) that we defined as the ratio of sample mass after contact (m_c) to fully soaked sample mass before contact (m_{sf}). The most severe lubricant depletion was measured for both nanoparticle coated fabrics, with a $\bar{m}_c$ of 0.8−0.85 and 0.8 after the 2 and 10 contact experiments, respectively. Multiplying the final normalized soaked mass of the samples ($\bar{m}_{sf}$) by $\bar{m}_c$ yields the ratio of masses of the fabric with retained oil to the dry fabric ($(m_{sf}/m_d)(m_c/m_{sf}) = mc/md$). For NP-cotton and NP-PET, this ratio (referred to as $\bar{m}_r$) was ∼1.4, implying that while these fabrics lose about half of the impregnated oil upon just 1 and 2 contacts (from a normalized soaked mass of 1.8), a large amount of the lubricant is retained within the fabric (about 0.4 fraction of dry fabric's mass). In contrast, after 10 contact experiments, the $\bar{m}_c$ ($\bar{m}_r$) was 0.97 (1.07), 0.96 (1.1), 0.86 (1.21), and 0.89 (1.1) for s-cotton, s-PET, i-cotton, and i-PET, respectively (see Figure 3A for all measured $\bar{m}_c$ values), so more oil was depleted from the i-fabrics than from the s-fabrics, whose oil retention was comparable to the PDMS slabs (compare left and right plots in Figure 3A). These results indicate that the fabrics modified with solid PDMS retain a higher fraction of the absorbed oil when brought into contact with the absorbing wipes. However, the PDMS modified fabrics also absorbed less of the oil during soaking (see Figure 1F) and, thus, in absolute terms had less stored oil when compared to the nanoparticle-coated fabrics, even after multiple contacts with the wipes. This difference likely stems from the oil occupying the space between fibers within the nanoparticle coated fabrics. In the case of the PDMS modified fabrics, the corresponding space can only be partially filled with oil because it is mostly occupied by the elastomer (oil is stored within this space when the elastomer swells with it). Storage of oil deep within the nanoparticle-coated fabrics could also explain why

DOI: 10.1021/am5085226
ACS Appl. Mater. Interfaces 2015, 7, 4224−4232

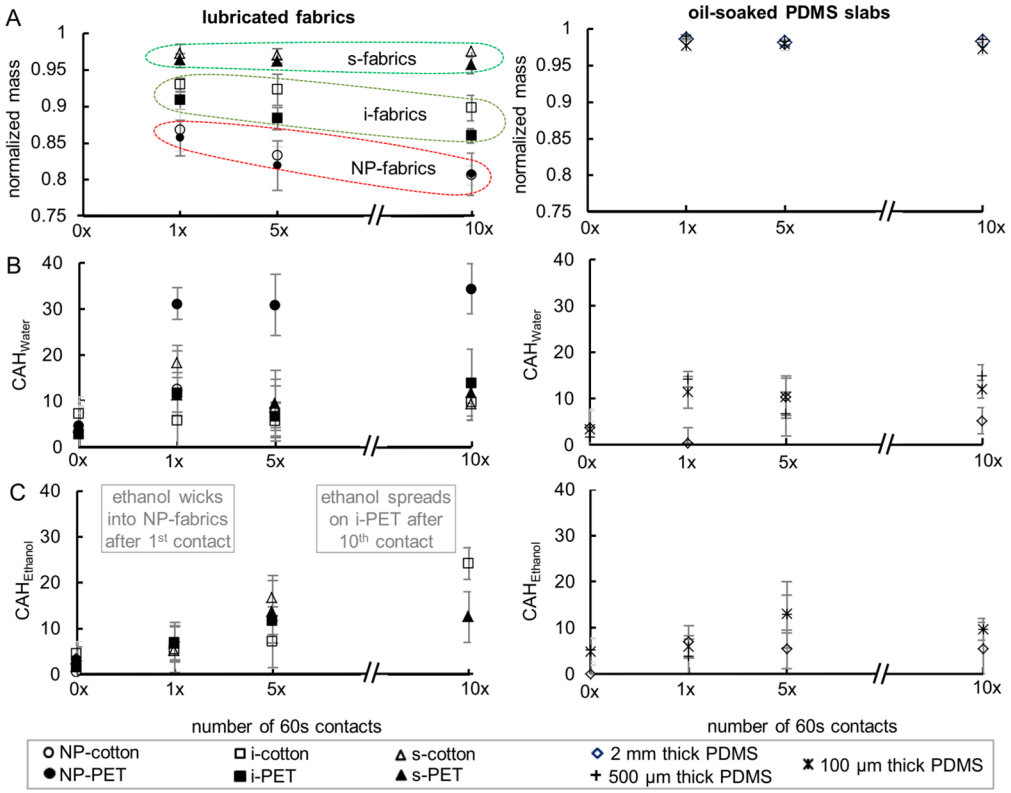

Figure 3. (A–C) Plots of (A) normalized mass after contact with wipes ($\bar{m}_c$), (B) water contact angle hysteresis (CAH), and (C) ethanol CAH for the six types of lubricated fabrics and, as reference, oil-soaked PDMS slabs with different thicknesses.

significant lubricant depletion from these samples occurs only during first and second contact with the wipes. The wipes during these initial contacts are likely to remove oil stored near the top and bottom surfaces, resulting in the formation of air cavities between the remaining oil and the exterior of the fabric. These air gaps below the surface of the NP-fabrics effectively shield the oil stored near the center of the NP-fabric from contact with subsequent wipes, explaining negligible oil loss after the second contact experiments.

Testing the wetting properties of specimens after contact with the absorbing wipes revealed dramatic changes. The plots in Figure 3B show that for the majority of the samples the water CAH increased from <10° to <20° after first contact with the wipes, but it remained unaffected by further contacts. The only exception was the NP-PET sample, which had the water CAH increase to ∼30°. The images in Figure 1C show that the polyester fibers were not as well coated by the hydrophobic nanoparticles as the cotton fibers and without the lubricant also had very large water CAH of ∼67° ± 4°. The plots in Figure 3C show that, for the ethanol experiments, not only did the CAH increase significantly but also the liquid wicked into the NP-fabrics after just a single pressurized contact with the absorbing wipes. This observation provides further evidence that contact with wipes depletes oil only near the top surface of the NP-fabrics (but some oil remains stored within the center of the fabrics after the first contact). As a result, ethanol can spread on textured fibers that are exposed at the surface. For the fabrics modified with solid PDMS prior to soaking in oil, the change in ethanol wetting was dependent on the fabric architecture. The surface of the s-fabrics, as well as all of the PDMS slabs, remained omniphobic even after 10 contact experiments. The minor increase of ethanol CAH on the s-fabrics and PDMS slabs from the initial ∼5° to below ∼15° was likely caused by a few crater-like surface imperfections that were exposed after oil depletion. In contrast, for the i-cotton, the CAH increased nearly linearly with the number of contacts, settling on ∼25° after the 10th contact (see left plot in Figure 3C). Moreover, the i-PET sample had a CAH below 10° after the first and the fifth contact experiments but was fully wetted by ethanol after the 10th contact experiments. As in the case of the nanoparticle coated fabrics, the change in wetting properties mostly correlates with values of the normalized mass after contact ($\bar{m}_c$): the wetting properties of the i-fabrics degrade as they lose oil near the surface, while the fabric-supported PDMS films, which retain a higher fraction of absorbed oil, remain omniphobic. Another factor contributing to the difference between the i- and s-fabrics is their different surface topology. The i-fabrics have topology closely following that of the underlying fabrics, while the s-fabrics are mostly flat. The i-fabrics take in more oil (see Figure 1F), which is absorbed into the polymer as well as stored between the topological features. However, as in the case of the lubricated nanoparticle-coated fabrics and solid textured materials,[30] the oil stored between the microscale topological features is most easily removed. Thus, despite the PDMS slowly releasing stored oil within its matrix, large microscale topological features are exposed by the contact experiments (see schematic in Figure 4A). As demonstrated by the strong pinning of water droplets on the partially delubricated i-cotton fabric highlighted in Figure 4A, the exposed topological features act as droplet pinning sites. Pinning by microscale topological features has also been previously observed for deposited[30] as well as condensed[26,31] droplets on solid nano/microtextured lubricated surfaces. In addition, we also observed water drop pinning on

DOI: 10.1021/am5085226
ACS Appl. Mater. Interfaces 2015, 7, 4224–4232

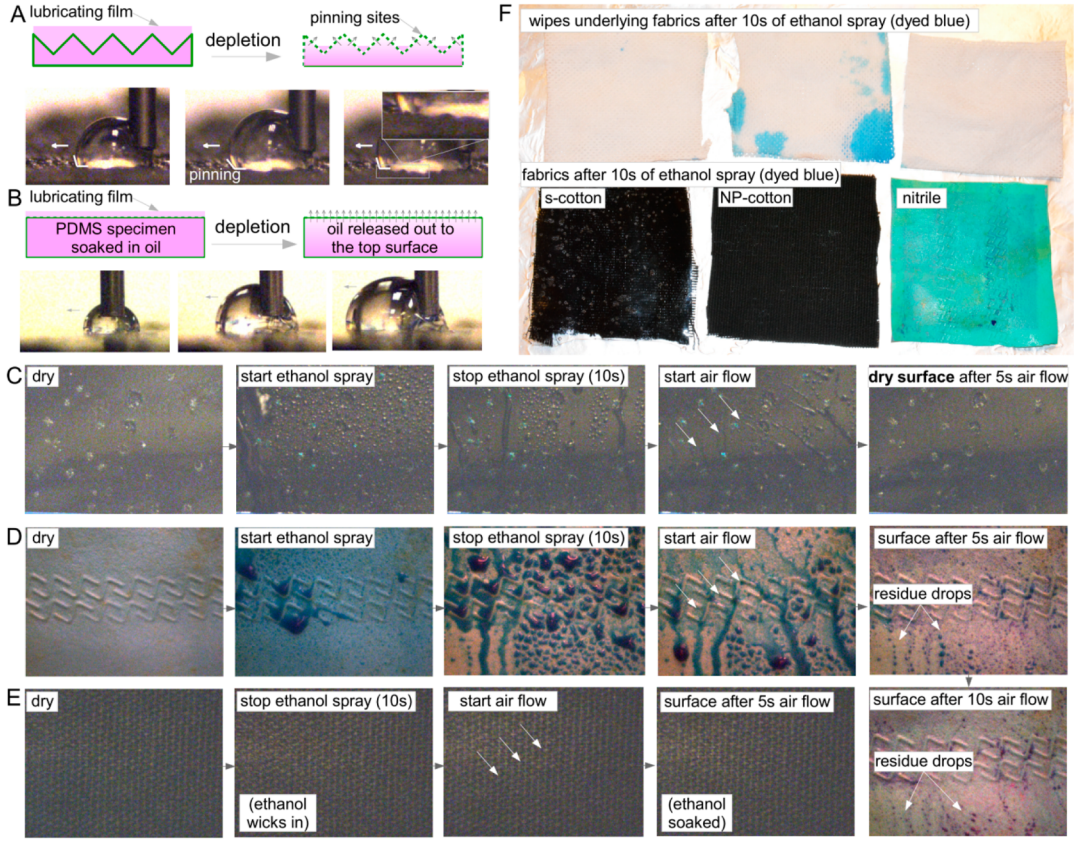

Figure 4. (A,B) Schematics of the oil depletion process and sequential images of the water droplet advancing on partially depleted (A) lubricated PDMS infused cotton fabric and (B) lubricated s-cotton fabric; (C–E) sequence of close-up images of large (~25 cm^2) samples of (C) lubricated s-cotton, (D) thick nitrile rubber used for personal protective gloves, and (E) lubricated NP-cotton during 5 s of ethanol spraying (dyed blue) followed by 5–10 s of a cleaning air flow step. Prior to spraying, the top surface of the lubricated fabrics was brought in contact with the absorbing wipe; (F) image showing fabrics and absorbing wipes that were underlying the three fabrics during the spraying experiments.

the i-fabrics prior to soaking in oil. We note that, when measuring the advancing contact angles, we selected the images of drops advancing and receding after relaxation from pinning, not at the rather sparse pinning site (separation of ~100–200 μm). In contrast, water drops advancing on the nearly smooth fabric supported PDMS films (i.e., s-fabrics) did not display any pinning (Figure 4B). Further, the fabric-supported PDMS films easily shed drops of ethanol even after 10 contact experiments because of the combination of a smooth surface and continual relubrication by oil that is released from the PDMS matrix. We observed nearly identical lubricant depletion and wetting trends for the contact experiments with 30 s contact intervals, details of which are presented in the Supporting Information.

To illustrate the potential of the best performing lubricated s-fabrics as omniphobic, durable, and easy to decontaminate personal protective gear, we sprayed larger (~25 cm^2) vertically mounted fabric samples with dyed ethanol mist for 5 s and tried to clean the liquid off from the samples using a moderate air flow. As reference, we also sprayed and attempted to air-dry a piece of a thick nitrile glove, which is a common component of personal protective gear. Before being mounted with tape, the lubricated samples were brought into contact with a large absorbing wipe under light pressure for 1 min. In addition, absorbing wipes with surface areas smaller than that of the fabrics were mounted under the samples before the start of the spraying experiments (for further details, see the Supporting Information). The images in Figure 4C,D show that, while ethanol droplets formed on the rubber and lubricated s-cotton samples, ethanol spread onto the lubricated NP-cotton sample. Furthermore, the image in Figure 4F shows that ethanol penetrated through the NP-cotton sample and stained the underlying wipe. In contrast, the s-cotton and nitrile samples not only prevented penetration of ethanol but also were cleaned from the majority of the deposited ethanol with moderate air flow. However, while 5 s of air flow was sufficient to entirely remove ethanol droplets from the s-cotton sample (i.e., completely dry surface), residual microdroplets of ethanol remained on the nitrile glove even after 10 s of air flow.

4. CONCLUSION

We have demonstrated that oil retention near the exterior surface as well as surface topology dictate whether lubricated fabrics remain omniphobic after contact with highly absorbing porous solids. Previously proposed nanoparticle coated fabrics remain hydrophobic but lose their omniphobic properties due to significant oil depletion near the fabric surface. This depletion is induced by a single, short, lightly pressurized contact with the absorbing wipe. In contrast, the oil-soaked fabrics modified with solid PDMS that swells with the oil lose less of the absorbed oil and consequently have more robust omniphobic characteristics. In addition, we demonstrated that the PDMS modified fabrics with flat rather than microtextured topology that followed the fabric weave performed significantly better, retaining most of their oil and remaining completely omniphobic even after 10 contact experiments (cumulative contact time with highly absorbing medium of 10 min). Our

DOI: 10.1021/am5085226
ACS Appl. Mater. Interfaces 2015, 7, 4224–4232

experiments also illustrated that the lubricated fabric supported PDMS films not only resist penetration of ethanol spray but that the ethanol can be completely removed with seconds of moderate airflow. While this work focused on the behavior of lubricated fabrics after contact with absorbing wipes, a few additional experiments presented in the Supporting Information section show that, at least in qualitative terms, the wetting dynamics of lubricated fabrics are similar after contact with wipes and with mimicked sand. In particular, after short contact with silica microparticle powder, NP-cotton was flooded by ethanol while s-cotton remained omniphobic.

Fabrication of the robust and durable omniphobic s-fabrics is simple and easily scalable. Their lubrication or relubrication can be done within ∼1.5 to 2 h, making them easy to maintain. Furthermore, selection of the fabric material can be used to tune the mechanical properties of the fabric as well as to provide an interesting option for active replenishment of the lubricant from the inside of the fabric via fiber wicking from a reservoir. Additionally, the lubrication time could be reduced by forcing pressurized lubricant from a syringe through the microfluidic network created within the slabs by the presence of the fabrics. A similar approach using microchannels embedded into a PDMS slab was recently found to increase biofouling resistance.[41] Thus, the introduced robust omniphobic fabrics could have applications as flexible materials for use as protection against hazardous biological and chemical liquids as well as easy to apply antifouling mats. Lastly, we note that PDMS and the silicone oil combination was used in this work to illustrate that polymers swollen with a lubricant could provide robust omniphobic surfaces. Naturally, the choice of the lubricant and the absorbing polymer, which can be designed to absorb the specific lubricant,[63] should be tuned to the specific application.

■ ASSOCIATED CONTENT

Supporting Information

Additional postfabrication images of PDMS modified fabrics, static and dynamic contact angle measurements, oil depletion, water and ethanol CAH after multiple 30 s interval contact experiments, control experiments with bare (unmodified) fabrics and s-NP-fabrics, lubricated fabric wetting properties after contact with mimicked sand, and specimen damage after bending and twisting. This material is available free of charge via the Internet at http://pubs.acs.org.

■ AUTHOR INFORMATION

Corresponding Author

*E-mail: konradr@asu.edu.

Author Contributions

⊥A.T., S.C., and C.K. contributed equally to this work.

Funding

K.R. acknowledges startup funding from the Ira A Fulton Schools of Engineering at Arizona State University. K.D. acknowledges the ASEE/NSF Small Business Postdoctoral Research Diversity Fellowship.

Notes

The authors declare no competing financial interest.

■ ACKNOWLEDGMENTS

We thank Dr. Sushant Anand from MIT for insightful comments and the LeRoy Eyring Center for Solid State Science at ASU for use of its electron microscopy facilities.

■ REFERENCES

(1) Gorzkowska-Sobas, A. A. *Chemical Warfare Agents and Their Interactions with Solid Surfaces*; Rapport 00574; Norwegian Defense Research Establishment: Kjeller, Norway, 2013.

(2) Center for Disease Control. *Infection Prevention and Control Recommendations for Hospitalized Patients with Known or Suspected Ebola Virus Disease in U.S. Hospitals*; available at http://www.cdc.gov/vhf/ebola/hcp/infection-prevention-and-control-recommendations.html (accessed Nov 1, 2014).

(3) Brevett, C. A.; Pence, J. J.; Nickol, R. G.; Maloney, E. L.; Myers, J. P.; Giannaras, C. V.; Sumpter, K. B.; King, B. E.; Hong, S. H.; Durst, H. *Evaporation Rates of Chemical Warfare Agents Measured Using 5 cm Wind Tunnels III. Munition-Grade Sulfur Mustard on Concrete*; DTIC Document; US Army: Aberdeen Proving Ground, MD, **2010**.

(4) Stebbins, A. A. Can Naval Surface Forces Operate Under Chemical Weapons Conditions? Master's Thesis, Naval Postgraduate School, Monterey, Calif., 2002.

(5) Gore, R. W.; Allen, S. B. Waterproof Laminate. US Patent 4,194,041, 1980.

(6) Zhang, J.; France, P.; Radomyselskiy, A.; Datta, S.; Zhao, J.; van Ooij, W. Hydrophobic Cotton Fabric Coated by a Thin Nanoparticulate Plasma Film. *J. Appl. Polym. Sci.* **2003**, *88*, 1473−1481.

(7) Lau, K. K. S.; Bico, J.; Teo, K. B. K.; Chhowalla, M.; Amaratunga, G. A. J.; Milne, W. I.; McKinley, G. H.; Gleason, K. K. Superhydrophobic Carbon Nanotube Forests. *Nano Lett.* **2003**, *3*, 1701−1705.

(8) Ma, M.; Mao, Y.; Gupta, M.; Gleason, K. K.; Rutledge, G. C. Superhydrophobic Fabrics Produced by Electrospinning and Chemical Vapor Deposition. *Macromolecules* **2005**, *38*, 9742−9748.

(9) Ma, M.; Gupta, M.; Li, Z.; Zhai, L.; Gleason, K. K.; Cohen, R. E.; Rubner, M. F.; Rutledge, G. C. Decorated Electrospun Fibers Exhibiting Superhydrophobicity. *Adv. Mater.* **2007**, *19*, 255−259.

(10) Zimmermann, J.; Reifler, F. A.; Fortunato, G.; Gerhardt, L.-C.; Seeger, S. A Simple, One-Step Approach to Durable and Robust Superhydrophobic Textiles. *Adv. Funct. Mater.* **2008**, *18*, 3662−3669.

(11) Gao, L.; McCarthy, T. J. "Artificial Lotus Leaf" Prepared Using a 1945 Patent and a Commercial Textile. *Langmuir* **2006**, *22*, 5998−6000.

(12) Wang, T.; Hu, X.; Dong, S. A General Route to Transform Normal Hydrophilic Cloths into Superhydrophobic Surfaces. *Chem. Commun.* **2007**, 1849−1851.

(13) Daoud, W. A.; Xin, J. H.; Tao, X. Superhydrophobic Silica Nanocomposite Coating by a Low-Temperature Process. *J. Am. Ceram. Soc.* **2004**, *87*, 1782−1784.

(14) Yu, M.; Gu, G.; Meng, W.-D.; Qing, F.-L. Superhydrophobic Cotton Fabric Coating Based on a Complex Layer of Silica Nanoparticles and Perfluorooctylated Quaternary Ammonium Silane Coupling Agent. *Appl. Surf. Sci.* **2007**, *253*, 3669−3673.

(15) Lafuma, A.; Quere, D. Superhydrophobic States. *Nat. Mater.* **2003**, *2*, 457−460.

(16) Quéré, D. Non-Sticking Drops. *Rep. Prog. Phys.* **2005**, *68*, 2495−2532.

(17) Cassie, A. B. D.; Baxter, S. Wettability of Porous Surfaces. *Trans. Faraday Soc.* **1944**, *40*, 546−551.

(18) Hoefnagels, H. F.; Wu, D.; de With, G.; Ming, W. Biomimetic Superhydrophobic and Highly Oleophobic Cotton Textiles. *Langmuir* **2007**, *23*, 13158−13163.

(19) Han, D.; Steckl, A. J. Superhydrophobic and Oleophobic Fibers by Coaxial Electrospinning. *Langmuir* **2009**, *25*, 9454−9462.

(20) Choi, W.; Tuteja, A.; Chhatre, S.; Mabry, J. M.; Cohen, R. E.; McKinley, G. H. Fabrics with Tunable Oleophobicity. *Adv. Mater.* **2009**, *21*, 2190−2195.

(21) Jung, Y. C.; Bhushan, B. Wetting Behavior of Water and Oil Droplets in Three-Phase Interfaces for Hydrophobicity/philicity and Oleophobicity/philicity. *Langmuir* **2009**, *25*, 14165−14173.

(22) Tuteja, A.; Choi, W.; Ma, M.; Mabry, J. M.; Mazzella, S. A.; Rutledge, G. C.; McKinley, G. H.; Cohen, R. E. Designing Superoleophobic Surfaces. *Science* **2007**, *318*, 1618−1622.

DOI: 10.1021/am5085226
ACS Appl. Mater. Interfaces 2015, 7, 4224−4232

(23) Tuteja, A.; Choi, W.; Mabry, J. M.; McKinley, G. H.; Cohen, R. E. Robust Omniphobic Surfaces. *Proc. Natl. Acad. Sci. U. S. A.* **2008**, 18200−18205.
(24) Srinivasan, S.; Chhatre, S. S.; Mabry, J. M.; Cohen, R. E.; McKinley, G. H. Solution Spraying of Poly(methyl methacrylate) Blends to Fabricate Microtextured, Superoleophobic Surfaces. *Polymer* **2011**, *52*, 3209−3218.
(25) Kota, A. K.; Kwon, G.; Tuteja, A. The Design and Applications of Superomniphobic Surfaces. *NPG Asia Mater.* **2014**, *6*, No. e109.
(26) Rykaczewski, K.; Paxson, A. T.; Staymates, M.; Walker, M. L.; Sun, X.; Anand, S.; Srinivasan, S.; McKinley, G. H.; Chinn, J.; Scott, J. H. J.; Varanasi, K. K. Dropwise Condensation of Low Surface Tension Fluids on Omniphobic Surfaces. *Sci. Rep.* **2014**, *4*, 4158.
(27) Wong, T.-S.; Kang, S. H.; Tang, S. K. Y.; Smythe, E. J.; Hatton, B. D.; Grinthal, A.; Aizenberg, J. Bioinspired Self-Repairing Slippery Surfaces with Pressure-Stable Omniphobicity. *Nature* **2011**, *477*, 443−447.
(28) Lafuma, A.; Quéré, D. Slippery Pre-Suffused Surfaces. *Europhys. Lett.* **2011**, *96*, 56001.
(29) Yao, X.; Hu, Y.; Grinthal, A.; Wong, T.-S.; Mahadevan, L.; Aizenberg, J. Adaptive Fluid-Infused Porous Films with Tunable Transparency and Wettability. *Nat. Mater.* **2013**, *12*, 529−534.
(30) Kim, P.; Kreder, M. J.; Alvarenga, J.; Aizenberg, J. Hierarchical or Not? Effect of the Length Scale and Hierarchy of the Surface Roughness on Omniphobicity of Lubricant-Infused Substrates. *Nano Lett.* **2013**, *13*, 1793−1799.
(31) Anand, S.; Paxson, A. T.; Dhiman, R.; Smith, J. D.; Varanasi, K. K. Enhanced Condensation on Lubricant-Impregnated Nanotextured Surfaces. *ACS Nano* **2012**, *6*, 10122−10129.
(32) Anand, S.; Rykaczewski, K.; Subramanyam, S. B.; Beysens, D.; Varanasi, K. K. How Droplets Nucleate and Grow on Liquids and Liquid Impregnated Surfaces. *Soft Matt.* **2014**, *11*, 69−80.
(33) Xiao, R.; Miljkovic, N.; Enright, R.; Wang, E. N. Immersion Condensation on Oil-Infused Heterogeneous Surfaces for Enhanced Heat Transfer. *Sci. Rep.* **2013**, *3*, 1988.
(34) Lalia, B. S.; Anand, S.; Varanasi, K. K.; Hashaikeh, R. Fog-Harvesting Potential of Lubricant-Impregnated Electrospun Nanomats. *Langmuir* **2013**, *29*, 13081−13088.
(35) Kim, P.; Wong, T.-S.; Alvarenga, J.; Kreder, M. J.; Adorno-Martinez, W. E.; Aizenberg, J. Liquid-Infused Nanostructured Surfaces with Extreme Anti-Ice and Anti-Frost Performance. *ACS Nano* **2012**, *6*, 6569−6577.
(36) Rykaczewski, K.; Anand, S.; Subramanyam, S. B.; Varanasi, K. K. Mechanism of Frost Formation on Lubricant Impregnated Surfaces. *Langmuir* **2013**, *29*, 5230−5238.
(37) Wilson, P. W.; Lu, W.; Xu, H.; Kim, P.; Kreder, M. J.; Alvarenga, J.; Aizenberg, J. Inhibition of Ice Nucleation by Slippery Liquid-Infused Porous Surfaces (SLIPS). *Phys. Chem. Chem. Phys.* **2013**, *15*, 581−585.
(38) Bengaluru Subramanyam, S.; Rykaczewski, K.; Varanasi, K. K. Ice Adhesion on Lubricant-Impregnated Textured Surfaces. *Langmuir* **2013**, *29*, 13414−13418.
(39) Zhu, L.; Xue, J.; Wang, Y.; Chen, Q.; Ding, J.; Wang, Q. Ice-Phobic Coatings Based on Silicon-Oil-Infused Polydimethylsiloxane. *ACS Appl. Mater. Interfaces* **2013**, *5*, 4053−4062.
(40) Epstein, A. K.; Wong, T.-S.; Belisle, R. A.; Boggs, E. M.; Aizenberg, J. Liquid-Infused Structured Surfaces with Exceptional Anti-Biofouling Performance. *Proc. Natl. Acad. Sci. U. S. A.* **2012**, *109*, 13182−13187.
(41) Howell, C.; Vu, T. L.; Lin, J. J.; Kolle, S.; Juthani, N.; Watson, E.; Weaver, J. C.; Alvarenga, J.; Aizenberg, J. Self-Replenishing Vascularized Fouling-Release Surfaces. *ACS Appl. Mater. Interfaces* **2014**, *6*, 13299−13307.
(42) Subramanyam, S. B.; Azimi, G.; Varanasi, K. K. Designing Lubricant-Impregnated Textured Surfaces to Resist Scale Formation. *Adv. Mater. Interfaces* **2014**, *1*, 1300068.
(43) Solomon, B. R.; Khalil, K. S.; Varanasi, K. K. Drag Reduction Using Lubricant-Impregnated Surfaces in Viscous Laminar Flow. *Langmuir* **2014**, *30*, 10970−10976.
(44) Eifert, A.; Paulssen, D.; Varanakkottu, S. N.; Baier, T.; Hardt, S. Simple Fabrication of Robust Water-Repellent Surfaces with Low Contact-Angle Hysteresis Based on Impregnation. *Adv. Mater. Interfaces* **2014**, *1*, 1300138.
(45) Smith, J. D.; Dhiman, R.; Anand, S.; Reza-Garduno, E.; Cohen, R. E.; McKinley, G. H.; Varanasi, K. K. Droplet Mobility on Lubricant-Impregnated Surfaces. *Soft Matter* **2013**, *9*, 1772−1780.
(46) Lee, C.; Kim, H.; Nam, Y. Drop Impact Dynamics on Oil-Infused Nanostructured Surfaces. *Langmuir* **2014**, *30*, 8400−8407.
(47) Carlson, A.; Kim, P.; Amberg, G.; Stone, H. Short and Long Time Drop Dynamics on Lubricated Substrates. *Europhys. Lett.* **2013**, *104*, 34008.
(48) Khalil, K. S.; Mahmoudi, S. R.; Abu-dheir, N.; Varanasi, K. K. Active Surfaces: Ferrofluid-Impregnated Surfaces for Active Manipulation of Droplets. *Appl. Phys. Lett.* **2014**, *105*, 041604.
(49) Boreyko, J. B.; Polizos, G.; Datskos, P. G.; Sarles, S. A.; Collier, C. P. Air-Stable Droplet Interface Bilayers on Oil-Infused Surfaces. *Proc. Natl. Acad. Sci. U. S. A.* **2014**, *111*, 7588−7593.
(50) Mruetusatorn, P.; Boreyko, J. B.; Venkatesan, G. A.; Sarles, S. A.; Hayes, D. G.; Collier, C. P. Dynamic Morphologies of Microscale Droplet Interface Bilayers. *Soft Matter* **2014**, *10*, 2530−2538.
(51) Shillingford, C.; MacCallum, N.; Wong, T.-S.; Kim, P.; Aizenberg, J. Fabrics Coated with Lubricated Nanostructures Display Robust Omniphobicity. *Nanotechnology* **2014**, *25*, 014019.
(52) Chinn, J.; Helmrich, F.; Guenther, R.; Wiltse, M.; Hurst, K.; Ashurst, R. W. Durable Super-Hydrophobic Nano-Composite Films. *NSTI-Nanotech* **2010**, *1*, 612−615.
(53) Rasband, W. S. ImageJ; http://rsb.info.nih.gov/ij/ (accessed Nov 1, 2014).
(54) Milne, A. Anti-Fouling Marine Compositions. US Patent 4,025,693, 1977.
(55) Callow, M. E.; Pitchers, R.; Santos, R. Non-biocidal anti-fouling coatings. In *Biodeterioration 7*; Springer: New York, 1988; pp 43−48.
(56) Edwards, D.; Nevell, T.; Plunkett, B.; Ochiltree, B. Resistance to Marine Fouling of Some Elastomeric Coatings of Poly-(dimethylsiloxanes) and Poly(dimethyldiphenyl-siloxanes). *Int. Biodeterior. Biodegrad.* **1994**, *34*, 349−359.
(57) Nevell, T.; Edwards, D.; Davis, A.; Pullin, R. The Surface Properties of Silicone Elastomers Exposed to Seawater. *Biofouling* **1996**, *10*, 199−212.
(58) Rice, S.; Diaz, A.; Minor, J.; Perry, P. Absorption of Silicone Oil by a Dimethylsiloxane Elastomer. *Rubber Chem. Technol.* **1988**, *61*, 194−204.
(59) Truby, K.; Wood, C.; Stein, J.; Cella, J.; Carpenter, J.; Kavanagh, C.; Swain, G.; Wiebe, D.; Lapota, D.; Meyer, A. Evaluation of the Performance Enhancement of Silicone Biofouling-Release Coatings by Oil Incorporation. *Biofouling* **2000**, *15*, 141−150.
(60) Kavanagh, C. J.; Swain, G. W.; Kovach, B. S.; Stein, J.; Darkangelo-Wood, C.; Truby, K.; Holm, E.; Montemarano, J.; Meyer, A.; Wiebe, D. The Effects of Silicone Fluid Additives and Silicone Elastomer Matrices on Barnacle Adhesion Strength. *Biofouling* **2003**, *19*, 381−390.
(61) MacCallum, N.; Howell, C.; Kim, P.; Sun, D.; Friedlander, R.; Ahanotu, O.; Hatton, B. D.; Wong, T. S.; Aizenberg, J. Liquid-Infused Silicone as a Biofouling-Free Medical Material. *ACS Biomater. Sci. Eng.* **2015**, *1*, 43−51.
(62) Verbraecken, J.; Van de Heyning, P.; De Backer, W.; Van Gaal, L. Body Surface Area in Normal-Weight, Overweight, and Obese Adults. A Comparison Study. *Metabolism* **2006**, *55*, 515−524.
(63) Ono, T.; Sugimoto, T.; Shinkai, S.; Sada, K. Molecular Design of Superabsorbent Polymers for Organic Solvents by Crosslinked Lipophilic Polyelectrolytes. *Adv. Funct. Mater.* **2008**, *18*, 3936−3940.

DOI: 10.1021/am5085226
ACS Appl. Mater. Interfaces 2015, 7, 4224−4232